On the Use of Quality Metrics to Characterize Structured Light-based Point Cloud Acquisitions

Tingcheng Li, Lou Ruding, Arnaud Polette, Nozais Dominique, Shao Zilong, Jean-Philippe Pernot

On the Use of Quality Metrics to Characterize Structured Light-based Point Cloud Acquisitions

Tingcheng Li[1], Ruding Lou[2], Arnaud Polette[1], Dominique Nozais[3], Zilong Shao[3], Jean-Philippe Pernot[1]

[1]Arts et Métiers Institute of Technology, LISPEN, HESAM Université, F-13617 Aix-en-Provence, France, tingcheng.li@ensam.eu, jean-philippe.pernot@ensam.eu, arnaud.polette@ensam.eu
[2]Arts et Métiers Institute of Technology, LISPEN, HESAM Université, F-71100 Chalon-sur-Saone, France, ruding.lou@ensam.eu
[3]Innovative - Manufacturing and Control, I-MC, Aix-en-Provence, France, dominique.nozais@i-mc.fr, zilong.shao@i-mc.fr

Corresponding author: Tingcheng Li, tingcheng.li@ensam.eu

Abstract. Even if 3D acquisition systems are nowadays more and more efficient, the resulting point clouds nevertheless contain quality defects that must be taken into account beforehand, in order to better anticipate and control their effects. Assessing the quality of 3D acquisitions has therefore become a major issue for scan planning. This paper presents several quality metrics that are then studied to identify those that could be used to optimize the acquisition positions to perform an automatic scan. From the experiments, it appears that, when considering multiple acquisition positions, the coverage ratio and score indicator have significant changes and can be used to evaluate the quality of the measurements. Differently, other indicators such as efficacy ratio, registration error and metrological characteristics are insensitive to some acquisition positions.

Keywords: Structured light scanning, Point cloud, Quality assessment, Quality metrics
DOI: https://doi.org/10.14733/cadaps.2023.1190-1203

1 INTRODUCTION

Accurately transferring the real world to the virtual one through reverse engineering is of utmost importance in Industry 4.0 applications. Indeed, acquiring good quality 3D representations of existing physical objects or systems has become crucial to maintain the coherence between a real object and its digital twin. Compared with traditional contact measurement, contact-less scanning is undoubtedly a fast and direct acquisition technology. However, for a given acquisition, finding the right scanning configuration (position, orientation, etc.) remains a challenging question whose resolution has attracted researchers in recent years. Using heuristics and visibility

criteria, some approaches try to automatically plan the positions and path to be followed by a robot when scanning an object being manufactured [7]. Similarly, Joe Eastwood et al. use a genetic algorithm and a convolutional neural network to optimize the locations of the cameras with the purpose that maximize surface coverage and measurement quality [3]. However, all those techniques base their reasoning on theoretical models whose real behavior may diverge as compared to real measuring. Thus, being able to take decisions based on the results obtained from real acquisitions is crucial to minimize the deviations between what was planned and what has been obtained by the end. To do so, ad-hoc metrics need to be used to accurately characterize the quality of point clouds that are then used in the next engineering steps (e.g. reconstruction, control, simulation).

The methods for evaluating point cloud (PC) quality can be divided into two types, i.e. subjective and objective. The former mainly evaluates the acquisition results from a human visual perception quality for immersive rendering of 3D contents [10][1], whereas the latter is based on more objective and quantitative characteristics that can be computed from the PC. Regarding quantitative metrics for quality assessment, some researchers only considered the properties of the PCs from four aspects [6]: noise, density, completeness and accuracy of the point cloud data. Based on these achievements, some scholars further proposed an indicator for surface accessibility, to characterize whether a surface region of the object can be reached or not by the scanner. Besides, the coverage rate was proposed to reveal how much of the object surface is covered. Additionally, the normal angle error was figured out in [1]. However, all those metrics can perform differently depending on the adopted technology: laser scanner, photogrammetry, or structured-light measurement. Catalucci et al. [2] compared the photogrammetry and structured-light measurements on additively manufactured parts and proposed PC quality indicators that include measurement performance indicators and statistical indicators on the whole part measurement. However, their work focused on entire scan of the part, consisting of many PCs acquired from different scan positions and configurations. Although many criteria have been proposed, it remains to be investigated which are the most accurate and obvious metrics to evaluate the quality of the point cloud during a structured light-based scanning.

This paper presents several quality metrics that are then studied to identify those that could be used to optimize the acquisition positions to perform an automatic scan. The contribution is twofold: (i) new metrics such as density, coverage and point-to-triangle dispersion to better capture possible artifacts, (ii) study of the metrics through several experiments using structured light-based acquisition system. Results show that the different metrics do not behave in the same way, and that some may be more interesting than others when optimizing the acquisition parameters. This can be of particular interest for path planning of the measuring system, thus enabling to automatically evaluate and optimize its positions.

The paper is organized as follows. Section 2 reviews the existing metrics and does introduce new ones. These metrics are then studied through several experiments detailed in section 3. The final section concludes this paper and discusses future works.

2 QUALITY METRICS

To assess the quality of point clouds, the metrics variants can be grouped according to the type of characteristics they refer to: inherent characteristics of point clouds, geometric characteristics and metrological characteristics as summarized in Table 1. Some of these metrics have been validated in the field of additively manufactured parts by Catalucci el. [2] on global scanning results where several point clouds are merged together after registration.

2.1 Inherent Characteristics of Point Clouds

This group of metrics focuses on the inherent characteristics of the point cloud. Catalucci et al. [2] validated some of them by comparing the results obtained on point clouds acquired by photogrammetry and structured-

Table 1: Metrics for evaluating the quality of PCs.

Type of characteristics	Metrics
Inherent characteristics	Number of raw points
	Number of final points
	Efficacy ratio
	Density
Geometric characteristics	Registration error
	Coverage ratio
	Normal error
Metrological characteristics	Point dispersion

light technologies. The metrics are as follows :

(a) Number of raw points, number of final points, and efficacy ratio:

Raw points are the points obtained from the acquisition device prior to any post-processing treatment, whereas final points refer to points that remain after post-processing (e.g. removing background, removing noise, registering, removing outliers). When the number of raw points is small, the scanning strategy is considered as not sufficiently efficient, and this may happen for instance when the position of the scanner is too close or too far from the object to be scanned, or when its material is too shinny. The efficacy ratio r_e is defined as the number of final points n_f divided by the number of original points n_r, following Eq. (1). The upper limit of this metric is 1.0, and the higher the efficiency ratio, the more efficient the acquisition is.

$$r_e = n_f / n_r \tag{1}$$

(b) Density:

The density is a metric that characterizes the number of points in a unit region. Two common configurations can be distinguished: one is the number of points per unit area, defined as Eq. (2), and the other is the number of points per unit volume as Eq. (3),:

$$D_s = n/S \tag{2}$$

$$D_v = n/V \tag{3}$$

where n, S and V are the count the of points in the neighborhood, the area of the neighborhood and the volume of the neighborhood respectively.

However, these definitions do not consider the spatial distribution of the points, thus limiting their capacity to distinguish configurations of equivalent density. As a consequence, a new metric is defined to better capture the local distribution of the points. The density D_l of a point P_c is defined in Eq. (4), where n_c is the number of points in the local neighborhood of P_c defined by a sphere of radius r centered on P_c, and d_i is the distance of the i^{th} point to the center point P_c, as shown in Fig. 1. Here, the spatial distribution is taken into account through the distance parameter d_i.

$$D_l = \begin{cases} \frac{log_{10}(n_c+9)}{n_c} \cdot \sum_{i=1}^{n_c} \frac{1}{d_i} & \text{if } n_c > 0 \\ 0 & \text{if } n_c = 0 \end{cases} \tag{4}$$

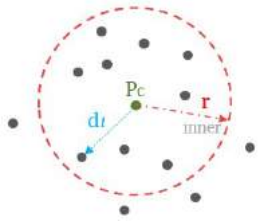

Figure 1: Density of the point P_c with searching radius r.

2.2 Geometric Characteristics of Point Clouds

The geometric characteristics consider the relationships between the acquired point cloud and a nominal geometric model, i.e. a CAD model in the context of this work. They take the registration process and the scan region into consideration.

2.2.1 Registration error

The registration error characterizes how well the point clouds coming from multiple acquisitions have been properly aligned in a common coordinate system by minimizing the alignment error [8]. Distances can be computed using either a point-to-point or a point-to-triangle computation strategy as Fig. 2 shows. The former' objective function is defined as Eq. (5), and the objective function of the point-to-plane registration is defined as Eq. (6), where R and t are optimization objectives, d_i and s_i a pair of corresponding points in the target and source sets, and the $\overrightarrow{n}_i$ the normal of d_i as shown in Fig. (3). The smaller the value, the better the quality of the alignment and therefore the better the quality of the point cloud is. In this work, the method point-to-triangle is used because researchers have observed significantly better convergence rates in the point-to-plane Iterative Closest Point (ICP) algorithm than that in point-to-point ICP algorithm [9].

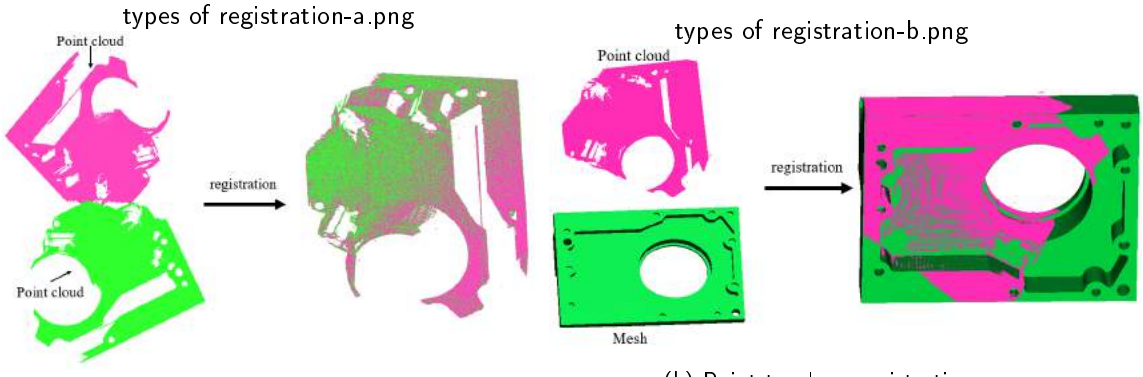

(a) Point-to-point registration.

(b) Point-to-plane registration.

Figure 2: Two registration strategies.

$$\mathbf{O}_{\text{pnt}} = \underset{R,t}{\operatorname{argmin}} \left\| \mathbf{d}_i - (\mathbf{R} \cdot \mathbf{s}_i + \mathbf{t}) \right\|_2^2 \tag{5}$$

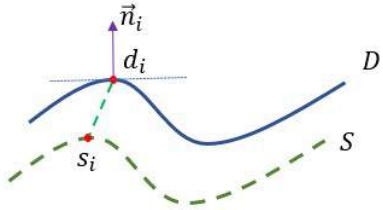

Figure 3: Registration optimization objective.

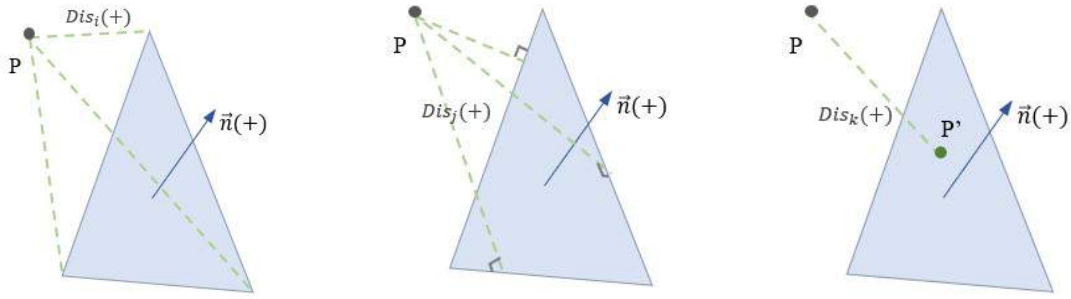

(a) Point-to-vertex. (b) Point-to-edge. (c) Point-to-face.

Figure 4: Point-to-triangle distance.

$$\mathbf{O}_{\text{pla}} = \underset{R,t}{\operatorname{argmin}} \left\{ \mathbf{n}_i^T \cdot [\mathbf{d}_i - (\mathbf{R} \cdot \mathbf{s}_i + \mathbf{t})] \right\}^2 \tag{6}$$

This metric is of interest to characterize the deviations between the acquired point cloud and known geometric model (i.e., B-Rep or mesh) of the part being scanned.

2.2.2 Point-to-triangle distance

Triangle mesh is a common geometric representation of the part, where triangle facets are used to describe its shapes. The continuous surface of the part is described by a piece-wise linear surface that is a discrete modelling for computer simulation. After a point cloud is registered, each acquired point can find a nearest facet by comparing its distances to the triangles in the mesh. The method of computing the distance between a point and a triangle is proposed in [4],[5]. The distance Dis from a point to a triangle can be divided into three cases as shown in Fig. 4: a) point-to-vertex distance, this distance is calculated between two points; b) point-to-edge distance, which is computed between the point P and its projection on the edge, and requiring that the projected point P' should be between the two vertexes of the edge; c) point-to-face distance, when the projection P' of point P lies on a face and the distance PP' is calculated. The value of the distance is the minimum absolute value of the three cases and the sign of distance (+/-) is related to the normal of the triangle of the mesh. As the Fig. 4 shows, if the point is on the side of the positive normal, the distance is considered positive (+), and negative (-) otherwise. This is used to calculate the coverage indicators in Section 2.2.3.

2.2.3 Coverage ratios

The coverage characterizes how much of the part surface on the geometric model is represented by the final point cloud. Here again, it is assumed that there exists a known model of the part being digitized. The coverage is computed from the results of the point-to-triangle distance. All indicators related to the coverage in this section are defined in [2] and work well in additive manufacturing, but it has not been explored on other manufacturing techniques. To deal with this problem in material removal manufacturing, remeshing on the digitized model is proposed to get uniform edge lengths, according to the scanner's resolution. In this paper, the edge length is 5 times bigger than the XY resolution of the adopted scanner. The metrics are as follows:

(a) **Number of points and area density corresponding to each triangle:**

This metric is associated to each triangle j of the triangle mesh corresponding to the CAD model of the scanned part. First, the number of points n^j_{pts} associated to the j-th triangle is computed. A point is considered to be associated to a triangle if the distance between the point and the triangle is less than a threshold Dis_r. Thus, area density d^j_{CA} of a triangle is the number n^j_{pts} divided by the area S^j of the triangle, as Eq. (7).

$$d^j_{CA} = n^j_{pts}/S^j \tag{7}$$

(b) **Covered, uncovered and zero triangle:**

If the area density of a triangle is bigger than a threshold T_C, the triangle is considered as covered. And if the area density is 0, the triangle is considered as a zero triangle, e.g. when the triangle is occluded. Otherwise, the triangle is considered as uncovered. The coverage status of a triangle j is computed by the Eq. (8). Uncovered triangle and zero triangle are completely different. If the triangle is uncovered, it means the region corresponding to the triangle is scanned, but not that much which may lead to inaccurate results when dealing for instance with fitting issues. If the triangle has a zero status, this means the facet is not scanned or could not be reconstructed during the scan.

$$status(j) = \begin{cases} covered, & d^j_{CA} > T_C \\ uncovered, & 0 < d^j_{CA} \leq T_C \\ zero, & d^j_{CA} = 0 \end{cases} \tag{8}$$

(c) **Coverage ratios:**

Two coverage ratios can be distinguished: the area ratio r_{CA} and the number ratio r_{CN}. These two ratios exploit Eq. (8) to know the status of the different triangles. The area ratio is the ratio of the total area of the covered triangles S_{cvd} to the theoretically covered area S_{Icvd}, i.e. the area of the region that can be theoretically seen in the field of the view of the scanner. Similarly, the number ratio is defined as the ratio of the number of covered triangles N_{cvd} to the number of theoretically covered facets N_{Icvd}:

$$r_{CA} = S_{cvd}/S_{Icvd} \tag{9}$$

$$r_{CN} = N_{cvd}/N_{Icvd} \tag{10}$$

2.2.4 Normal error

Each covered facet j has a normal $\vec{n}^j_f$, and the points associated to this facet are characterized by a normal $\vec{n}^j_p$ computed from the best fit with a plane, as shown in Fig. 5. The two vectors should theoretically be the same, but they usually differ. The normal error E^j_n of a triangle j measures the deviation in terms of angle

between the two vectors. It is defined as Eq. (11). If the angle θ^j between the normals is small, the E_n^j will also be small.

$$E_n^j = 1 - \left| \frac{\vec{n}_f^j \cdot \vec{n}_p^j}{\left\|\vec{n}_f^j\right\| \cdot \left\|\vec{n}_p^j\right\|} \right| \tag{11}$$

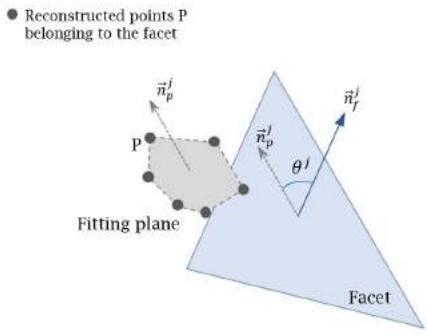

Figure 5: Deviation between the normal to a triangle j, and the normal to the plane fitting the points covering this triangle.

2.3 Metrological Characteristics

These metrics reflect accuracy of scan in the measurement, including point-to-triangle dispersion, and dimensional accuracy of fitting features (e.g. length, width, and height). Different from the indicators proposed in [2], the new point-to-triangle dispersion x_j for the j-th facet is defined with Eq. (12), where n_{pts}^j is the number of points related to the j-th facet through coverage algorithm, and the Dis_k^j is the point-to-triangle distance between the k-th points covering the j-th triangle. As Fig. 6 shows, the projected distance should be 0 under ideal cases and the dispersion indicates the fitting precision. Considering a complete scanned region, the distribution of the dispersion has three characteristics: mean $\bar{x}$, standard deviation σ and range R, computed by Eq. (13), where n_T is the number of triangles in the scanned region. In addition, the accuracy on the sizes of some features can be defined as the deviation between the fitting value and the real one.

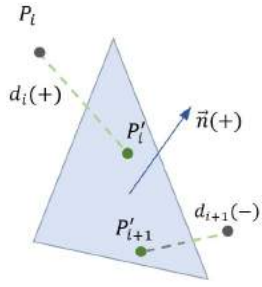

Figure 6: Point-to-face dispersion for a facet j.

$$x_j = \sqrt{\frac{1}{n_{pts}^j} \sum_{k=1}^{n_{pts}^j} (Dis_k^j)^2} \tag{12}$$

$$\begin{cases} \bar{x} = \frac{1}{n_T} \sum_{j=1}^{n_T} x_j \\ \sigma = \sqrt{\frac{1}{n_T} \sum_{j=1}^{n_T} (x_j - \bar{x})^2} \\ R = [\min(x_j), \max(x_j)] \end{cases} \tag{13}$$

3 COMPARATIVE STUDY ON METRICS

3.1 Experiment Workbench and Data Processing

The experiments have been performed using the structured light-based GOCATOR 3210 by LMI Technologies as shown in Fig. 7. To study the way the previously introduced metrics behave on different scan configurations, the pocket workpiece shown in Fig. 8 has been scanned while changing the acquisition viewpoint on a rotating table (acquisition angles of $0°$, $10°$, $20°$ and $40°$). The VDI/VDE accuracy and XY-plane resolution of the scanner can reach 0.034mm and 0.06mm-0.09mm respectively.

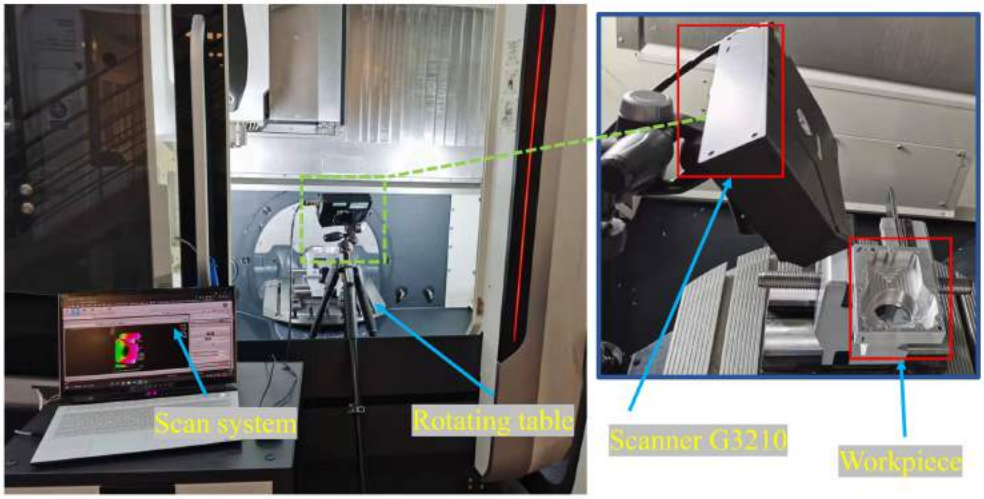

Figure 7: Point cloud acquisition setup.

Data processing includes the removal of the background related to the surrounding environment near the workpiece, removal of the outliers and isolated points and registration between the point cloud and CAD model. In this paper, the background was deleted manually first. Then the registration was done following a point-to-plane strategy. Meanwhile, outliers were deleted. Finally, isolated points were deleted by density analysis defined in Section 2.1. The density in the ideal case shown in the Fig. 9 shall be over 9.023 calculated by the Eq. 4 with the search radius $r = 0.3$mm (the search radius r is set to 3 times bigger of the scanner resolution, here 0.09 + 0.01 mm). The threshold for cleaning isolated points is set to the 50% of the ideal density.

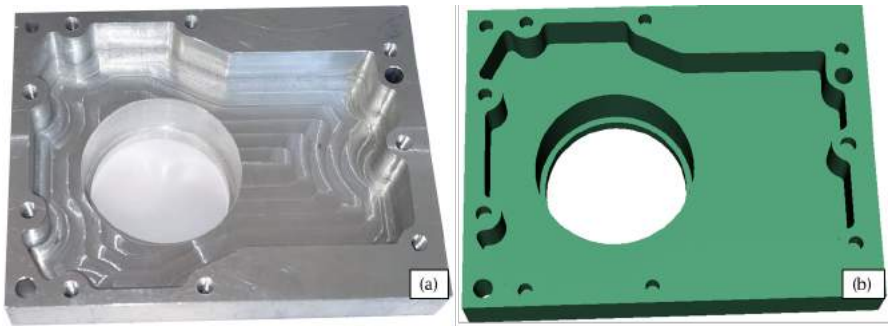

Figure 8: The pocket workpiece and its CAD.

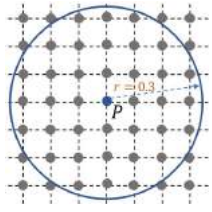

Figure 9: Ideal density.

3.2 Use of Metrics

The metrics not only reveal the quality of the point clouds, but also some of them can be used to indicate quality of the scan configuration, i.e. to evaluate whether the scanner has been set up and positioned appropriately.

3.2.1 Inherent characteristics of point clouds

First, metrics related to the inherent characteristics are analyzed. The results of the numbers of raw points, final points, and efficacy ratio of the four acquisitions on the pocket are listed in Table 2, where we can conclude that the efficacy ratio is stable. Besides, the densities of the four scans of the pocket workpiece are shown in Fig. 10. Even though the density distribution of the acquisition at position 10° is different from the others with low mean density, the values do not vary significantly and the efficacy ratio has little change. Thus, those metrics are not able to finely capture differences between acquisitions and would therefore be less interesting for optimizing scan configurations.

Table 2: Efficacy ratio metric of the pocket's scans

Position	Num of raw PC	Num of final PC	Efficacy ratio
0^o	1439322	1389531	96.54%
10^o	460229	444295	96.54%
20^o	1155815	1114418	96.42%
40^o	1434403	1388178	96.78%

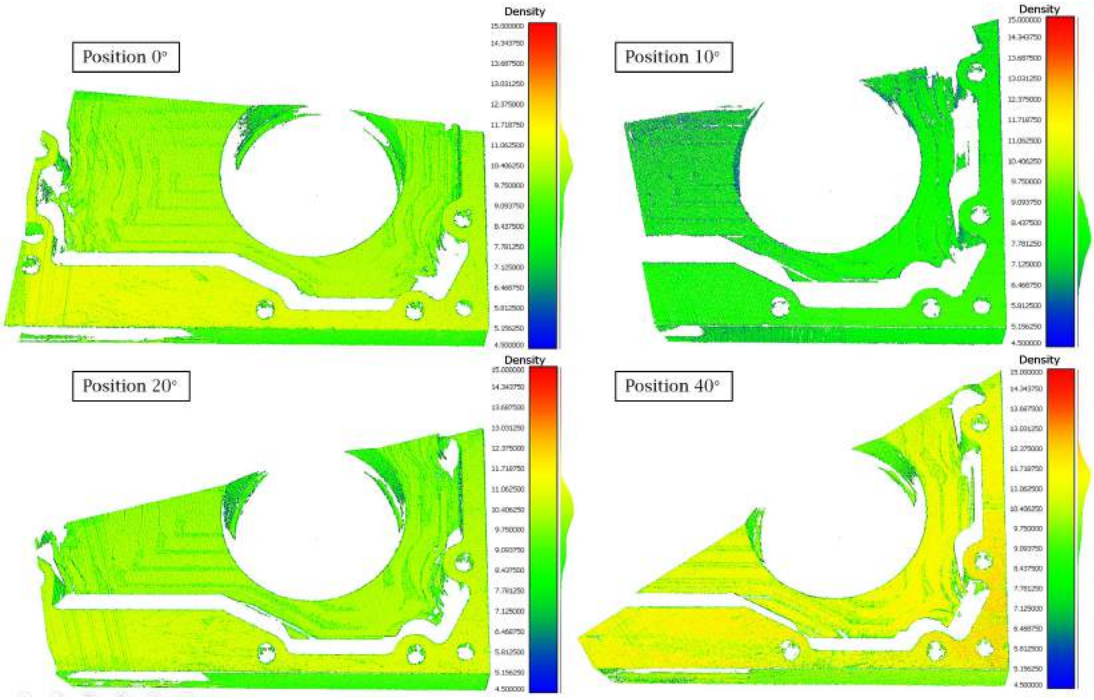

Figure 10: Densities of point clouds for 4 positions of the pocket.

3.2.2 Geometric characteristics of point clouds

Metrics related to the geometric characteristics of the point clouds are then analyzed. All these indicators are related to the CAD model of the pocket, thus the CAD model are remeshed by MeshLab with an edge length of 0.5mm. And this will make the coverage area ratio r_{CA} and coverage number ratio r_{CN} be equivalent. Thus, only the coverage number ratio r_{CN} is the used, because of its lower computation cost when compared to r_{CA}.

Table 3: Registration error of the pocket's PCs

Position	Registration error
0^o	0.074mm
10^o	0.075mm
20^o	0.075mm
40^o	0.075mm

The registration errors are listed in Table 3. For the four acquisitions, the registration errors have little changes, varying from 0.074mm to 0.075mm. Here again, it can be noticed that those values do not vary and that therefore such a metric can hardly be used as an objective function to be minimized. Besides, this step offers normalized data for the following point cloud evaluation metrics.

The coverage of each of the four scans of the pocket are shown in Fig. 11, where coverage status of

Table 4: Coverage ratio and $Score$ of 4 scans from the pocket.

Position	Num of theoretical covered facets N_I	Num of covered facets N_C	Num of uncovered facets N_{uc}	Coverage ratio r_{CN}	$Score$
0^o	86769	66345	8234	76.46%	4.48
10^o	78131	40522	12449	51.86%	1.98
20^o	72276	55357	7539	76.59%	4.29
40^o	80716	50221	5210	62.22%	4.22

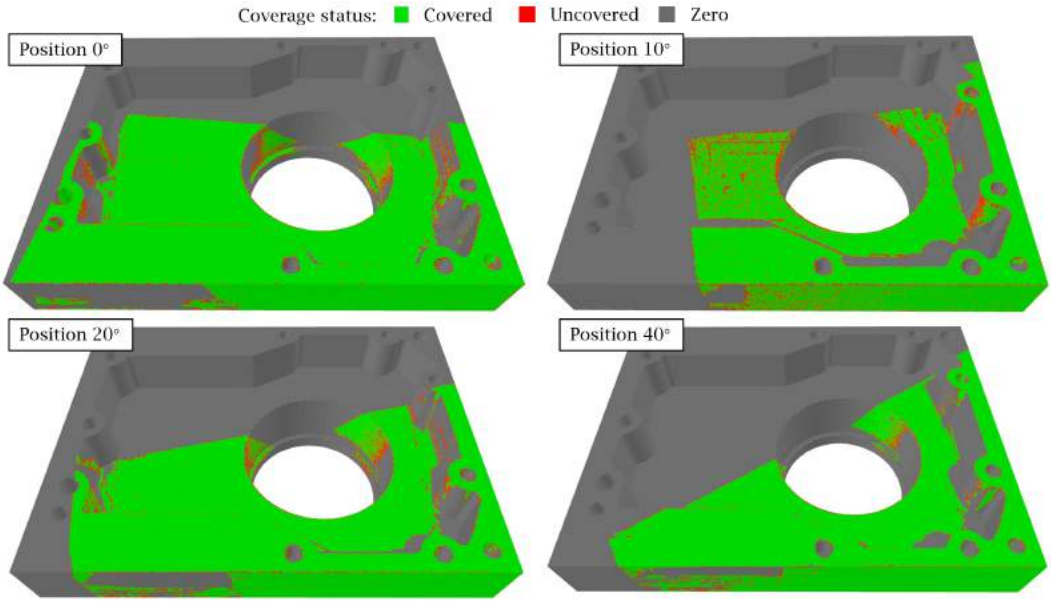

Figure 11: Coverage of scans.

Table 5: The statistics of the dispersions of the pocket.

Position	mean	std.dev	Range
0^o	0.055	0.044	[0, 0.209]
10^o	0.056	0.040	[0, 0.209]
20^o	0.055	0.042	[0, 0.209]
40^o	0.060	0.041	[0, 0.210]

each facet is computed considering the number of points associated to the facet as defined in Eq. (8): (a) covered (green); (b) uncovered (red); (c) zero (grey). Detailed values are summarized in Table 4.

In order the better capture the sensitivity of the coverage ratio, a new indicator is proposed as Eq. (14) where N_C, N_I and N_{UC} are respectively the number of the covered triangles, the theoretical covered and the

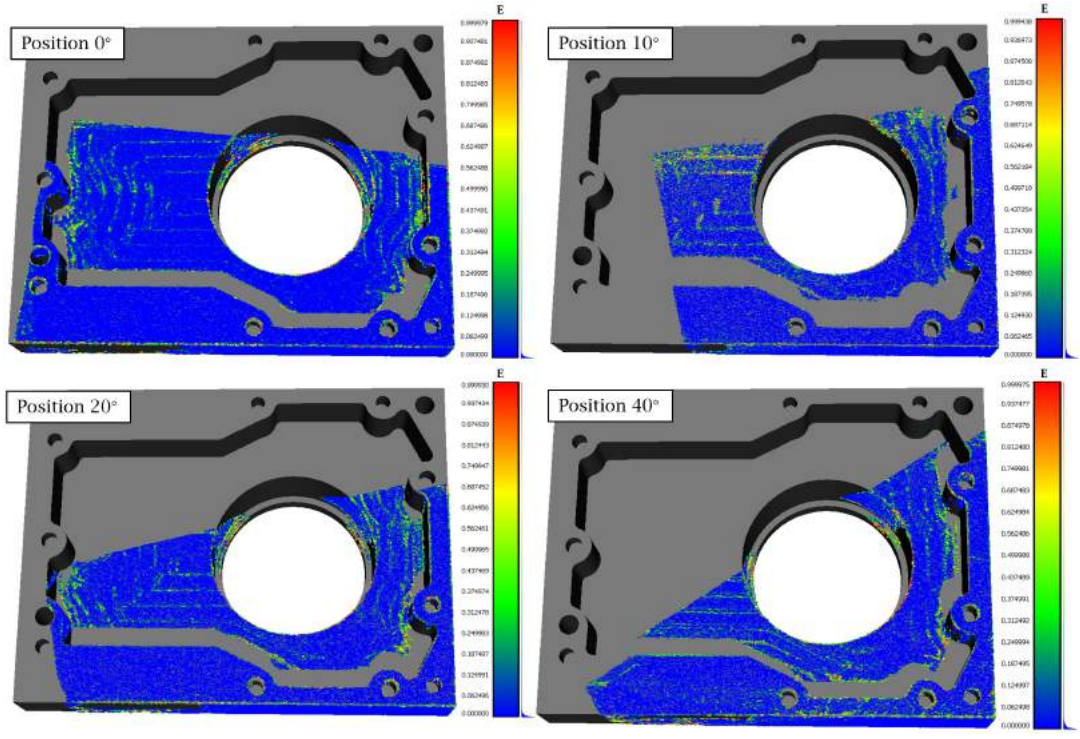

Figure 12: Normal error of the four scans.

uncovered.

$$Score = \exp\left(\frac{N_C}{N_I}\right) \cdot \ln\left(\frac{N_C}{N_{UC}}\right) \tag{14}$$

This indicator considers both the coverage ratio and the ratio between the covered and the uncovered. Actually, it can be seen as the signal-to-noise ratio when the covered triangles are treated as noise. The bigger it is the better it is.

From the results, it is obvious that the PC at position $10°$ has low score on coverage and it is consistent with the fact that this PC has a higher percentage of uncovered area than the other PCs. Thus, $Score$ indicator can capture differences between scan configurations, and could therefore be used as a metric to be maximized when looking for optimal scan configuration/position.

The four acquisitions are also analysed on the normal error between the fitting normal and corresponding one from CAD mesh shown in Fig. 12. It is noticed that the indicator of the four scans has a close distribution so this metric is not sensitive enough to be used to optimize scan configuration.

3.2.3 Metrological characteristics of point clouds

The dispersion of each triangle is shown in Fig. 13 and the statistics of the several scans are analyzed in Table 5. The results on the dispersion distribution of the point clouds show very similar results that, again, do not allow for a good comparison of scan configurations. This metric is therefore not a good candidate for scan configuration optimization.

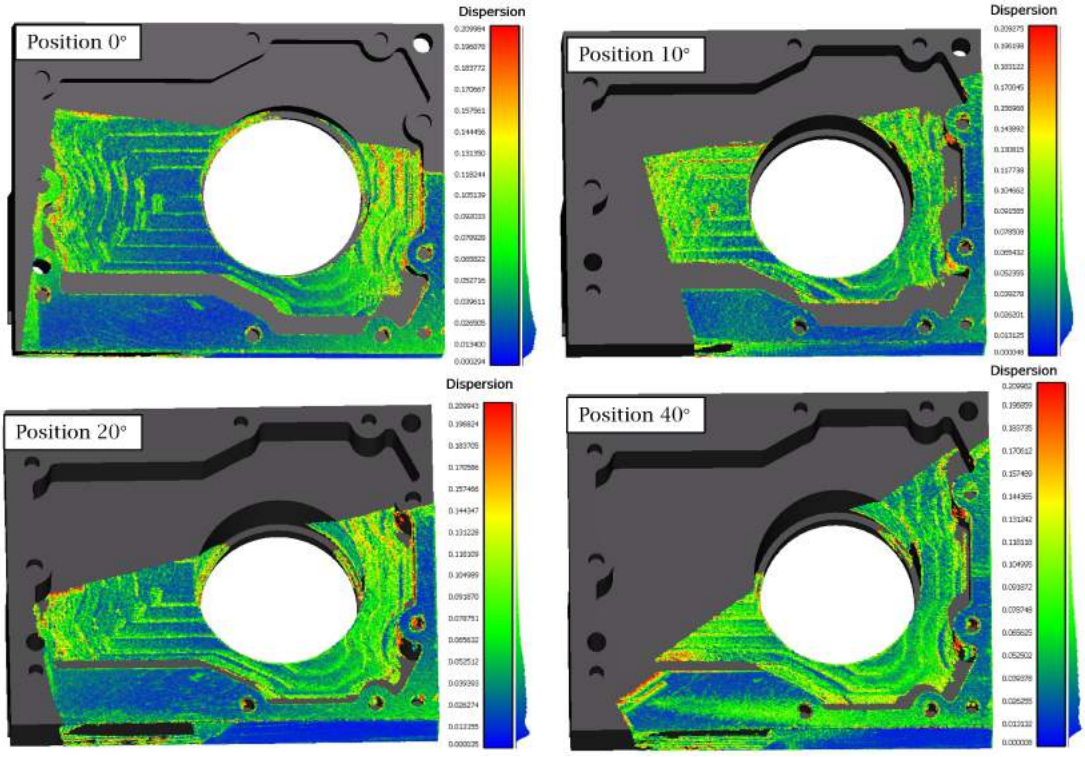

Figure 13: Dispersions of 4 PCs of the pocket.

4 CONCLUSIONS

Metrics for evaluating the quality of point clouds are studied with the aims of optimizing scanning path to realize automatic scanning. Firstly, the indicators based on the inherent characteristics of the point clouds are summarized and the new density considering spatial distribution is proposed. Then, considering the geometric characteristics of point clouds corresponding to the model, coverage indicators are analyzed after registration. Finally, the dispersion is considered. The study reveals that the indicators number of points, number of covered/uncovered triangles vary greatly, and may be affected by external factors (such as the location and configurations of the device). Other indicators such as the efficacy ratio, registration error and metrological characteristics keep stable and are therefore not interesting to get a good understanding of the pertinence of some acquisition positions. However, the indicators coverage ratio and score have significant changes and can be of interest to assess the quality of the measurements. Besides, since the scanner used in this study is based on structured-light technology, these conclusions remain valid for other structured-light acquisition systems.

ACKNOWLEDGEMENTS

This work was supported by the China Scholarship Council (No. 202006830012) and the Innovative - Manufacturing and Control (I-MC) company.

Tingcheng. Li, http://orcid.org/0000-0001-8304-8699
Ruding. Lou, http://orcid.org/0000-0002-4395-2154

Arnaud. Polette, http://orcid.org/0000-0002-8572-6454
Dominique. Nozais, http://orcid.org/000-0000-1234-5678
Zilong. Shao, http://orcid.org/0000-0003-0042-9862
Jean-Philippe. Pernot, http://orcid.org/0000-0002-9061-2937

REFERENCES

[1] Alexiou, E.; Ebrahimi, T.: On subjective and objective quality evaluation of point cloud geometry. In Ninth International Conference on Quality of Multimedia Experience, QoMEX 2017, Erfurt, Germany, May 31 - June 2, 2017, 1–3. IEEE, 2017. http://doi.org/10.1109/QoMEX.2017.7965681.

[2] Catalucci, S.; Senin, N.; Sims-Waterhouse, D.; Ziegelmeier, S.; Piano, S.; Leach, R.: Measurement of complex freeform additively manufactured parts by structured light and photogrammetry. Measurement, 164, 108081, 2020.

[3] Eastwood, J.; Zhang, H.; Isa, M.; Sims-Waterhouse, D.; Leach, R.; Piano, S.: Smart photogrammetry for three-dimensional shape measurement. In Optics and Photonics for Advanced Dimensional Metrology, vol. 11352, 113520A. International Society for Optics and Photonics, 2020.

[4] Eberly, D.: Distance between point and triangle in 3d. Magic Software, http://www. magic-software. com/Documentation/pt3tri3. pdf, 1999.

[5] Georgiades, P.N.: Signed distance from point to plane. In D.B. Kirk, ed., Graphics Gems III (IBM Version), The Graphics Gems Series, 223–224. Academic Press, 1992. http://doi.org/10.1016/b978-0-08-050755-2.50050-6.

[6] Lartigue, C.; Contri, A.; Bourdet, P.: Digitised point quality in relation with point exploitation. Measurement, 32(3), 193–203, 2002.

[7] Peuzin-Jubert, M.; Polette, A.; Nozais, D.; Mari, J.; Pernot, J.: Survey on the view planning problem for reverse engineering and automated control applications. Comput. Aided Des., 141, 103094, 2021. http://doi.org/10.1016/j.cad.2021.103094.

[8] Pomerleau, F.; Colas, F.; Siegwart, R.: A review of point cloud registration algorithms for mobile robotics. Found. Trends Robotics, 4(1), 1–104, 2015. http://doi.org/10.1561/2300000035.

[9] Rusinkiewicz, S.; Levoy, M.: Efficient variants of the icp algorithm. In Proceedings third international conference on 3-D digital imaging and modeling, 145–152. IEEE, 2001.

[10] Zhang, J.; Huang, W.; Zhu, X.; Hwang, J.: A subjective quality evaluation for 3d point cloud models. In International Conference on Audio, Language and Image Processing, ICAILP 2014, Shanghai, China, July 7-9, 2014, 827–831. IEEE, 2014. http://doi.org/10.1109/ICALIP.2014.7009910.